Models of the elastic x-ray scattering feature for warm dense aluminum

C. E. Starrett and D. Saumon
Los Alamos National Laboratory, P.O. Box 1663, Los Alamos, New Mexico 87545, USA
(Received 28 May 2015; published 3 September 2015)

The elastic feature of x-ray scattering from warm dense aluminum has recently been measured by Fletcher *et al.* [Nature Photonics **9**, 274 (2015)] with much higher accuracy than had hitherto been possible. This measurement is a direct test of the ionic structure predicted by models of warm dense matter. We use the method of pseudoatom molecular dynamics to predict this elastic feature for warm dense aluminum with temperatures of 1–100 eV and densities of 2.7–8.1 g/cm^3. We compare these predictions to experiments, finding good agreement with Fletcher *et al.* and corroborating the discrepancy found in analyses of an earlier experiment of Ma *et al.* [Phys. Rev. Lett. **110**, 065001 (2013)]. We also evaluate the validity of the Thomas-Fermi model of the electrons and of the hypernetted chain approximation in computing the elastic feature and find them both wanting in the regime currently probed by experiments.

DOI: 10.1103/PhysRevE.92.033101 PACS number(s): 52.25.Os, 52.27.Gr, 52.38.−r

I. INTRODUCTION

X-ray scattering is a powerful probe of dense plasmas of approximately solid density and temperatures of a few to hundreds of eV. Such states of matter are known as warm dense matter (WDM) and occur during the implosion of inertial confinement fusion capsules and in dense astrophysical objects such as giant gaseous planets and white dwarf stars. X-ray scattering experiments on WDM states have largely focused on the study of the inelastic electron feature [the "Compton feature" and plasmon peak(s)] caused by free electrons in the plasma and in some cases, bound-free transitions [1–7]. Several experiments probed the elastic ion feature to measure the ion structure factor in warm dense plasmas [8,9] but did not effectively constrain theoretical models of WDM. More recently, the characteristics of x-ray free electron lasers and the development of a novel experimental technique has enabled accurate measurements of the elastic ion feature in x-ray spectra [10]. The latter is directly proportional to the ion-ion static structure factor $S_{\rm II}(k)$ and contains information about, but is less sensitive to, the electron density around a nucleus from both bound and screening electrons. Studies of the elastic scattering peak promise to be a sensitive and informative test of the ionic structure of the plasma and to a lesser extent of the structure of the screening cloud predicted by warm dense matter models.

The first experimental determination of the elastic scattering feature for warm dense aluminum by Ma *et al.* [11] showed a large peak indicative of very strong ion-ion correlations. However, subsequent modeling of the experimental conditions with several independent methods [12–14] predicted an ion-ion correlation peak about half as large as measured. Very recently a second experimental measurement of $S_{\rm II}(k)$ for aluminum by Fletcher *et al.* [10] also observed a strong ion-ion correlation peak but, crucially, at a plasma temperature and density significantly different from those of the earlier experiment [11]. In this paper, we show that the method which we call pseudoatom molecular dynamics (PAMD) [12] agrees very well with the more recent data [10], in stark contrast to the disagreement with the former experiment of Ref. [11]. We demonstrate that the method [12,15] indicates that the two experiments reach states of widely different plasma coupling, and thus significant differences in the amplitude of the first peak in $S_{\rm II}(k)$ are expected, contrary to the experimental results.

Furthermore, we use recent experimental data [10] to demonstrate the inadequacy of two approximations that are often used in models of WDM. We first investigate the hypernetted chain (HNC) approximation, which is used to close the integral equations of fluid theory. Given the ion-ion interaction pair potential $V_{\rm II}(r)$, ion number density $n_{\rm I}^0$, and inverse temperature $\beta = 1/k_{\rm B}T$, the static structure of the ions is uniquely determined by the Ornstein-Zernike (OZ) equation

$$h_{\rm II}(r) = c_{\rm II}(r) + n_{\rm I}^0 \int d\boldsymbol{r}'\, c_{\rm II}(r') h_{\rm II}(|\boldsymbol{r} - \boldsymbol{r}'|) \qquad (1)$$

and a closure relation

$$g_{\rm II}(r) = \exp[-\beta V_{\rm II}(r) + h_{\rm II}(r) - c_{\rm II}(r) + B_{\rm II}(r)]. \qquad (2)$$

In these expressions, $h_{\rm II}(r)$ is the pair correlation function, $c_{\rm II}(r)$ is the direct correlation function, and $g_{\rm II}(r) = h_{\rm II}(r) + 1$ is the pair distribution function. The ion-ion static structure factor is related to the Fourier transform of the pair correlation function

$$S_{\rm II}(k) = 1 + n_{\rm I}^0 \int d\boldsymbol{r}\, e^{i\boldsymbol{k}\cdot\boldsymbol{r}} h_{\rm II}(r). \qquad (3)$$

The so-called bridge function $B_{\rm II}(r)$ is not determined by these equations and is difficult to calculate. The HNC approximation consists of setting $B_{\rm II}(r) = 0$, which has been shown to work well for the one-component plasma model (OCP) [16,17] but is of uncertain accuracy for describing WDM states. We show that the variational modified HNC (VMHNC) approximation [18,19], where the bridge function is approximated by that of hard spheres, yields excellent agreement with the "exact" molecular dynamics simulations using the same potential, and in turn with the recent experiment [10].

The second approximation we consider is the Thomas-Fermi (orbital-free) form of density functional theory (DFT) used to compute the electronic structure of the plasma. With this approximation, the PAMD model fails to reproduce the data while PAMD with Kohn-Sham DFT agrees very well with the experiment [10]. From a theoretical perspective neither of these results is surprising, but to our knowledge, this is the first time they have been demonstrated in warm dense matter by

direct comparison to an experiment which measures the ionic structure.

In Sec. II we review PAMD, its key approximations, current state of validation, and where it is expected to break down. We also demonstrate that the VMHNC approximation gives excellent agreement with corresponding classical MD simulations given the same ion-ion pair interaction potential, for an aluminum plasma. In Sec. III we compare the PAMD predictions of the elastic scattering feature to the recent experiment of Fletcher *et al.* We show the inadequacy of the HNC and TF approximations. We also revisit the experiment of Ma *et al.,* focusing on the variation of the PAMD prediction with plasma temperature.

II. SUMMARY OF THE PAMD MODEL

The key assumption of PAMD is that the electron density of a dense plasma $n_e(\boldsymbol{r})$ can be accurately approximated as a superposition of identical, spherically symmetric pseudoatom electron densities $n_e^{\text{PA}}(r)$, placed at each nuclear site, i.e.,

$$n_e(\boldsymbol{r}) = \sum_i n_e^{\text{PA}}(|\boldsymbol{R}_i - \boldsymbol{r}|), \tag{4}$$

where $\boldsymbol{R}_i$ is the position vector of nucleus i, and the sum runs over all nuclear sites. The generalization to mixtures is straightforward [20].

The key quantity is therefore the pseudoatom electron density $n_e^{\text{PA}}(r)$. This is calculated in an average atom framework [21] using DFT, for which both orbital-based (Kohn-Sham) and orbital-free versions of PAMD are possible and have been explored. Clearly the Kohn-Sham version should be more physically realistic for a wider range of conditions than current orbital-free formulations. At higher temperatures and densities one expects and finds that both models converge to the same equation of state and ionic structure [15,22]. Regardless of which DFT version is used, $n_e^{\text{PA}}(r)$ is calculated with only the mass density, temperature, nuclear charge, and mass as input. There are no adjustable parameters. For all calculations presented here we have used a finite temperature, local density approximation for the exchange and correlation potential [23]. Furthermore, all calculations are performed in thermodynamic equilibrium with the electrons at the same temperature as the ions.

The ion-ion interaction potential $V_{\text{II}}(r)$ is evaluated numerically from the pseudoatom electron density $n_e^{\text{PA}}(r)$ [15]. This potential is then used to determine the ionic configurations and dynamics using classical molecular dynamics (MD) simulations. Alternatively, if only the static ionic properties are of interest, $V_{\text{II}}(r)$ can be used in the integral equations of fluid theory [Eqs. (1) and (2)]. Together with an additional approximation for the bridge function (such as HNC or VMHNC), quantities like the ion-ion pair distribution function and structure factor can be calculated very efficiently. In Fig. 1 we compare the static structures for an aluminum plasma at 6.3 g/cm^3 obtained with MD[1] and the Ornstein-Zernike (OZ) equations with the bridge function derived from the VMHNC

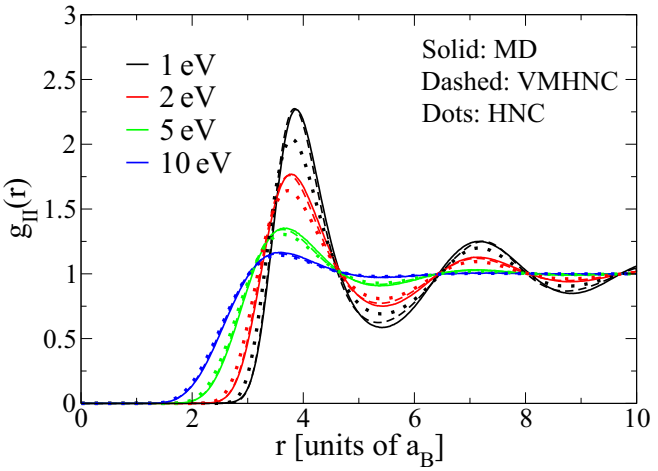

FIG. 1. (Color online) Ion-ion pair distribution functions $g_{\text{II}}(r)$ for aluminum at 6.3 g/cm^3 for a range of temperatures. All results are Kohn-Sham PAMD calculations using either classical molecular dynamics (MD) or the integral equations of fluid theory (the Ornstein-Zernike equations) to determine $g_{\text{II}}(r)$ from the same $V_{\text{II}}(r)$. For the latter we show results using both the hypernetted chain (HNC) and the variational modified HNC (VMHNC) approximations for the bridge function. VMHNC is an excellent approximation to the "exact" MD result up to very strong coupling regimes, and the dashed and solid lines overlap almost perfectly.

formalism [18]. For these conditions, the plasma ranges from moderately to strongly coupled, as can be seen from the significant structure in $g_{\text{II}}(r)$. The comparison demonstrates the quality of the VMHNC approximation to $B_{\text{II}}(r)$, with the classical MD giving the nominally "exact" solution for a given potential $V_{\text{II}}(r)$. Clearly, the VMHNC model is very accurate, even for very strongly coupled plasmas, and can be relied upon as a practical and inexpensive substitute to a MD calculation of static ion properties. On the other hand, the HNC approximation ($B_{\text{II}}(r) = 0$) becomes rather poor for $T \lesssim 5$ eV, which corresponds to an effective OCP plasma coupling parameter of $\Gamma_{\text{OCP}}^{\text{eff}} \gtrsim 20$ (see Table I).

PAMD can be characterized as an approximate version of DFT-MD, which is widely considered to be the best tool available today to model WDM. PAMD has been validated against DFT-MD [15,20,22], giving generally good to excellent agreement on static ($g_{\text{II}}(r)$, $S_{\text{II}}(k)$) and dynamic properties (self-diffusion coefficient) and thermodynamics as well. However, the method is not expected to work everywhere. In regimes where chemical bonding occurs (typically, low temperature and relatively low densities) the superposition approximation (4) becomes invalid [20]. Thus our validation studies have borne out that PAMD works well for dense, simple plasmas. The advantage of PAMD over the corresponding DFT-MD method is that it is much more computationally efficient, allowing extensive exploration of temperature and density space, as well as access to quantities that may be

[1]For the MD simulations we used 1000 particles and 6000 production time steps following 20 000 equilibration steps where velocity scaling was used to achieve the target temperature. The length of the time step depends on the temperature and is determined with the method proposed in Ref. [24].

TABLE I. Effective plasma coupling parameter for Al plasmas extracted from the PAMD pair distribution functions using the method of Ref. [26]. The fourth column gives the reference to corresponding experiments. The rapid decrease in $\Gamma_{\rm OCP}^{\rm eff}$ from 1 to 20 eV at for all densities indicates a transition from a strongly to a moderately coupled fluid.

T(eV)	ρ (g/cm^3)	$\Gamma_{\rm OCP}^{\rm eff}$	Experiment
2	2.7	29.2	
5	2.7	8.1	
10	2.7	4.7	
20	2.7	3.6	
50	2.7	3.9	
100	2.7	4.0	
1	6.3	130.9	
1.75	6.3	69.7	[10]
2	6.3	60.1	
5	6.3	17.0	
10	6.3	8.2	
2	8.1	66.8	
5	8.1	19.3	
10	8.1	9.2	[11]
20	8.1	5.7	
50	8.1	5.1	
100	8.1	5.1	

sensitive to the smaller system sizes that are typical of DFT-MD simulations [25]. Moreover, the nature of the underlying model can clarify the physical nature of dense plasmas.

III. PREDICTIONS OF $W(k)$ AND COMPARISONS WITH EXPERIMENTS

In x-ray scattering experiments the static elastic contribution $W(k)$ to the measured electron-electron dynamic structure factor can be approximated as [12,27,28]

$$W(k) = [f(k) + q(k)]^2 S_{\rm II}(k), \tag{5}$$

where $f(k)$ and $q(k)$ are the form factors of the bound and screening electrons, respectively. In the PAMD model this is just the Fourier transform of the pseudo-atom electron density $n_e^{\rm PA}(k) = f(k) + q(k)$.

Recently Fletcher *et al.* measured $W(k)$ in warm dense aluminum [10]. Analysis of the plasmon peak of the x-ray spectrum indicates that the sample was compressed to 6.3 g/cm^3 at 1.75 eV [10]. We compare predictions from the PAMD model, using the Kohn-Sham version and the VMHNC approximation to the bridge function, to the data and find remarkably good agreement (Fig. 2), especially since the calculation is not fitted to the data in any way. Equation (5) shows that $W(k)$ is a simple product of $S_{\rm II}(k)$ and $[n_e^{\rm PA}(k)]^2$. Charge neutrality of the pseudoatoms requires that $n_e^{\rm PA}(k=0) = 13$, the charge of the Al nucleus. Furthermore, Fig. 2 shows that $n_e^{\rm PA}(k)$ is a slowly decaying function of k. Thus $W(k)$ reflects the overall shape of the static structure factor, with a peak corresponding to the first peak in $S_{\rm II}(k)$ and decaying to zero at large k (Fig. 2).

For small k the PAMD result lies at the upper edge of the experimental result. Since $n_e^{\rm PA}(k)$ is close to its $k = 0$ limit,

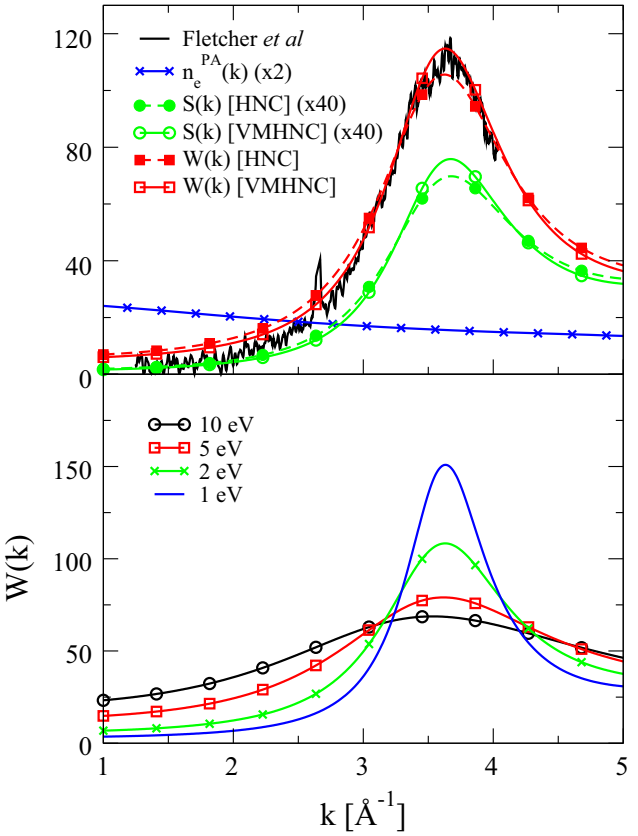

FIG. 2. (Color online) Elastic x-ray scattering feature $W(k)$ for aluminum at 6.3 g/cm^3. In the top panel the Kohn-Sham PAMD result using VMHNC is compared to the experimental measurement at 1.75 eV [10], with very good agreement. On the other hand, the HNC approximation does not agree as well. The contributions to $W(k)$ [Eq. (5)], $S_{\rm II}(k)$ and $n_e^{\rm PA}(k)$ are also shown (scaled). The bottom panel shows how $W(k)$ obtained with the Kohn-Sham PAMD with VMHNC evolves with temperature.

this suggests that the PAMD calculation slightly overestimates $S_{\rm II}(k=0)$ for these conditions. Perhaps the PAMD ion-ion potential is slightly too soft, which would most likely come from the superposition approximation [Eq. (4)]. This would result is a more compressible plasma and a higher $S_{\rm II}(k=0)$. This low-k discrepancy may be related to the tendency of PAMD to overestimate the adiabatic sound speed in warm dense Al [25]. Figure 2 also shows $S_{\rm II}(k)$ and $W(k)$ calculated with PAMD using the HNC approximation [$B_{\rm II}(r) = 0$]. The agreement with the data is good, but somewhat worse than the VMHNC result. The peak of the $W(k)$ is on the lower edge of the data and is also broader, resulting in a noticeably worse agreement in the $k = 2$–3 Å^{-1} range.

Fletcher *et al.* [10] obtain an excellent agreement with their data with a model dubbed "HNC-Y+SRR" [29] that involves a parametric $V_{\rm II}(r)$ that is adjusted to match results from DFT-MD simulations [30]. This is in contrast to the PAMD method, where $W(k)$ is obtained without inputs from external calculations. While both models agree very well with the data, there is an important qualitative difference in their sensitivity to temperature. In the lower panel of Fig. 2 we show $W(k)$ for temperatures of 1–10 eV at the experimental

density of 6.3 g/cm^3. The PAMD calculation indicates that the peak of $W(k)$ decreases rapidly with increasing temperature. The temperature dependence of $W(k)$ in the PAMD calculation comes almost entirely from variations in $S_{II}(k)$, because $n_e^{PA}(k)$ depends only very weakly on temperature for the k values probed by the experiment. On the other hand, the HNC-Y+SRR model predicts that $W(k)$ is nearly independent of temperature for the same conditions [10]. The temperature dependence of the ionic structure as predicted by PAMD has been found to be in agreement with KS-DFT-MD simulations [22] under similar conditions. A measurement of $W(k)$ for aluminum using the method of [10] but at a higher temperature (say, 5 eV) would clarify the situation.

The amplitude of the first peak of $S_{II}(k)$ is indicative of the strength of the coupling between the ions. In an OCP this is quantified with the plasma coupling parameter

$$\Gamma = \frac{Z^2 e^2}{a k_B T}, \tag{6}$$

where Z is the ion charge, e the quantum of charge, and a the ion sphere radius. The plasma is considered strongly coupled when $\Gamma \gg 1$. At a fixed density (as in Fig. 2 and Fig. S3 of Ref. [10]), a is constant, and for $T = 1$ to 10 eV, the charge of Al ions is very nearly constant at $Z = 3$ [10,11,31]. Thus Γ should decrease by a factor of $\sim$10 when T increases from 1 to 10 eV. Unlike in the OCP model, the ion-ion potential in the plasmas of interest here are not purely Coulombic, but an electron-screened potential with a repulsive core. Nevertheless, we can map the characteristics of the calculated $g_{II}(r)$ to that of an OCP to obtain an effective coupling parameter that gives a more intuitive sense of the strength of coupling in the real plasma. For this purpose, we use a mapping based on the height of the first peak of $g_{II}(r)$ and the radius r_{12} where $g_{II}(r_{12}) = 0.5$ [26] for the OCP (inverse screening length $\kappa = 0$). Table I gives the values of $\Gamma^{\rm eff}_{\rm OCP}$ obtained from the PAMD $g_{II}(r)$ for the various Al plasmas shown in this publication. As expected, the coupling is about one order of magnitude weaker at 10 eV than at 1 eV, in broad agreement with the simple OCP picture, and supporting the qualitative temperature dependence of the PAMD results. For each density listed in Table I, $\Gamma^{\rm eff}_{\rm OCP}$ reaches a plateau at high temperature that reflects the competition between increased temperature, which reduces the plasma coupling, and increasing ionization, which increases $\Gamma^{\rm eff}_{\rm OCP}$ [32,33].

In contrast to this good agreement with the experimental measurement of $W(k)$ of Fletcher *et al.* (Fig. 2), the same PAMD model leads to a strong disagreement [12] with the measurement of Ma *et al.* [11], who report $W(k)$ also for Al but at a higher temperature (10 eV) and somewhat higher density (8.1 g/cm^3). As with the Fletcher *et al.* data, the HNC-Y+SRR model was found to agree very well with the results of Ma *et al.* [11]. However, two independent DFT-MD simulations failed to agree [13,14] with the data of [11] and confirmed the PAMD result. References [14,34] showed that the Ma *et al.* $W(k)$ could be reproduced by lowering the ion temperature well below the electron temperature of 10 eV derived from the inelastic peak of the x-ray spectrum. In Fig. 3 we revisit the comparison of PAMD calculations with the Ma et al. data. For $T \sim$ 2–3 eV, the PAMD model recovers the strong peak and

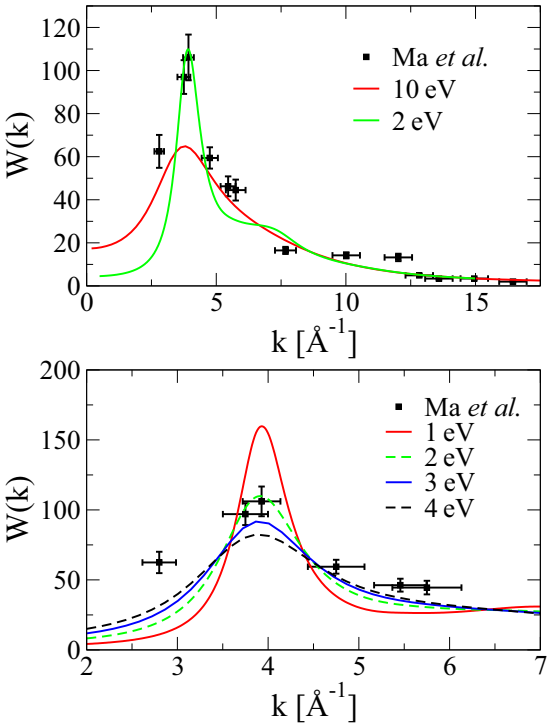

FIG. 3. (Color online) Comparison of the elastic peak $W(k)$ calculated with Kohn-Sham PAMD using VMHNC with the aluminum data of Ma *et al.* [11]. The state of the plasma is reported to be 8.1 g/cm^3 and 10 eV, for which the PAMD calculation strongly disagrees with the data near the peak [12]. In the bottom panel we focus on the peak region. The experimental peak height can be recovered with PAMD by lowering the temperature to $\sim$2 3 eV. The small bump at $k \sim 7$ Å^{-1} corresponds to the second peak in $S_{II}(k)$.

overall fit of $W(k)$ obtained in Ref. [14]. Taken at face value, this suggests a plasma that is far from equilibrium, where the electron temperature $\sim$10 eV and the ion temperature $\sim$2 eV. However, this is hard to reconcile with estimates of the equilibration time scale, which is very short [14,34].

Table I shows that the different experimental conditions result in very different coupling strengths, primarily due to the factor of $\sim$6 higher temperature in the Ma *et al.* experiment. In light of these results, it is surprising that both experiments measure a peak value of $W(k) \sim 110$.

Finally, all the calculations of $W(k)$ shown in Fig. 3 underestimate the measurement at the lowest wave vector $k = 2.8$ Å^{-1}. For the temperatures that provide the best match to the peak height of $W(k)$ (2–3 eV), PAMD comes about a factor of two under the measurement. All other published modelizations of this data [11–14,34] display, to varying degrees, a faster drop toward small k than is indicated by the data. As a point of reference, our $W(k)$ agrees very well with that of Ref. [13] (their Fig. 3) obtained with KS-DFT-MD for 8.1 g/cm^3 and $T = 10$ eV. The PAMD models shows that the form factor $(f(k) + q(k))^2$ is nearly independent of temperature for $T =$ 1–10 eV. On the other hand, the plasma is more strongly coupled and less compressible at lower T so $S(k = 0)$ decreases, hence the steady drop of $W(k = 2.8$ Å$^{-1})$ seen in Fig. 4 as T decreases. It is surprising that four different

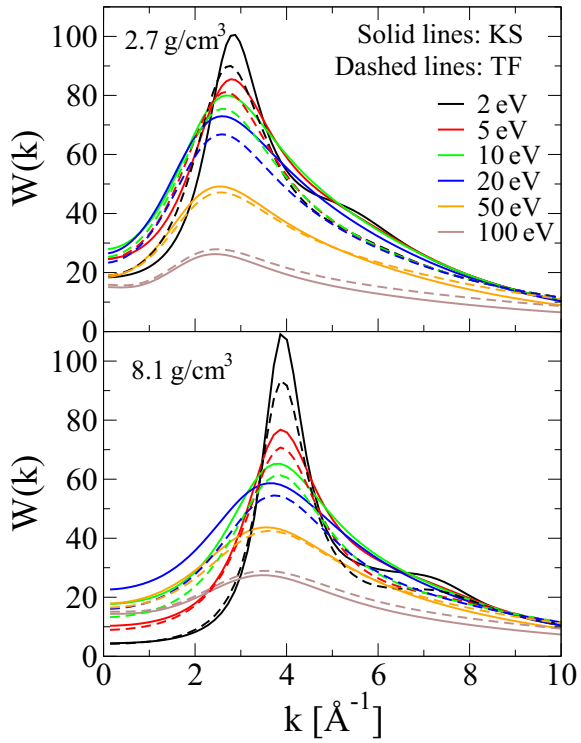

FIG. 4. (Color online) Behavior of $W(k)$ as a function of temperature for aluminum at solid density (2.7 g/cm^3; top panel) and three times solid density (8.1 g/cm^3; bottom panel), as predicted by PAMD using the VMHNC approximation. Calculations with both the orbital-based Kohn-Sham (KS) DFT (solid lines) and orbital-free, Thomas-Fermi (TF) DFT (dashed lines) are shown.

approaches to computing $W(k)$ would fail to match this data point.

In Fig. 4 we use PAMD to predict $W(k)$ up to 100 eV for aluminum at solid and three times solid density. At the lowest temperatures we observe a strong peak indicative of a strongly coupled fluid, with $W(k)$ being more sharply peaked for the higher density, as expected. Increasing the temperature greatly reduces the height and increases the width of the peak, which is characteristic of a transition towards a moderately to weakly coupled plasma. For the higher temperatures ($\gtrsim$50 eV) the peak height is also suppressed by a reduction in $n_e^{\rm PA}(k)$ due to the larger screening length and increased ionization of the plasma.

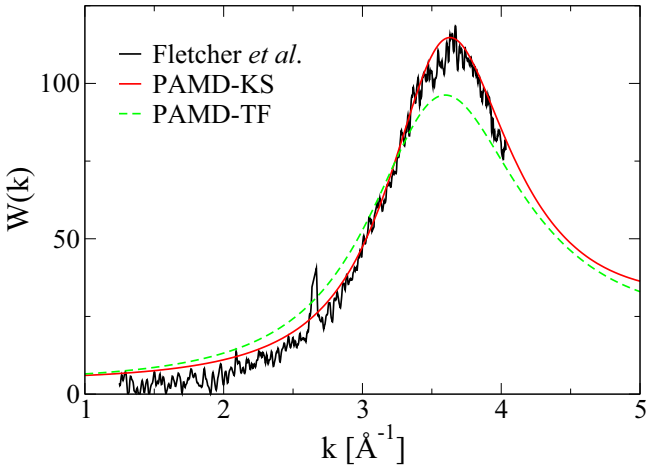

FIG. 5. (Color online) $W(k)$ as calculated with PAMD using both Kohn-Sham (KS) and Thomas-Fermi (TF) DFT, compared to the experiment of Ref. [10], for aluminum at 6.3 g/cm^3 and 1.75 eV. The high signal-to-noise ratio of the experiment reveals the inadequacy of the TF-based calculations.

Also shown in the figure are the results of orbital-free PAMD calculations using the Thomas-Fermi functional. The differences with the Kohn-Sham calculations of $W(k)$ are substantial at low temperature. As expected, agreement improves at higher temperatures and the distinction becomes small for $\gtrsim$50 eV. In Fig. 5 we contrast Kohn-Sham and Thomas-Fermi PAMD prediction for $W(k)$ under the experimental conditions [10] and compare to the measured data. The quality of the data clearly reveals that the Thomas-Fermi approach is an inadequate approximation under these conditions.

IV. CONCLUSIONS

We have used pseudoatom molecular dynamics to calculate the elastic feature of x-ray scattering in warm dense aluminum over a wide range of conditions ($T = 1$ to 100 eV, $\rho = 1$–3 times solid density) that correspond to regimes of very strong to modest plasma coupling. We present calculations where the static ionic structure is evaluated with classical molecular dynamics (the "MD" of PAMD) as well as with the Ornstein-Zernike equations using the HNC and VMHNC approximations to the bridge function. The high quality of the VMHNC approximation is demonstrated for realistic plasma potentials[2] in the warm dense matter regime through comparison with "exact" MD results for the same ion-ion pair potential. We also investigated the effect on $W(k)$ of describing the ions and their screening electron clouds with the Kohn-Sham and Thomas-Fermi versions of density functional theory.

A direct comparison with a recent experiment on strongly coupled aluminum [10] shows good agreement with the data when using the VMHNC and the Kohn-Sham models. On the other hand the same model confirms earlier analysis of another experiment [11] on moderately coupled warm dense aluminum: The peak of the elastic feature can only be reproduced with an ion temperature that is a factor of ~4–5 lower than the derived electron temperature. Our detailed modeling is supported by simple physical arguments about the strength of ion coupling in the two experimental plasmas. We conclude that the earlier experimental results [11] remain incompatible with the current and two other [13,14] theoretical calculations, while the more recent experiment [10] validates the present approach.

We also show that two popular approximations in modeling warm dense matter must be used with caution for calculating $W(k)$. The HNC approximation for the Ornstein-Zernike equations becomes poor for effective coupling corresponding

[2]Excellent results using VMHNC have also been obtained for Lennard-Jones systems [35], the Yukawa-OCP [19], and liquid metals [36].

to $\Gamma_{\rm OCP}^{\rm eff} \gtrsim 20$ and gives a marginal fit to the data for Fletcher *et al.* For aluminum plasmas of roughly solid density, the Thomas-Fermi model of the electrons becomes reliable only for $T \gtrsim 50$ eV. It is a very promising prospect for studies of WDM that data on the elastic feature can be obtained with enough accuracy to clearly distinguish between these models.

ACKNOWLEDGMENTS

We are grateful to L. B. Fletcher and S. H. Glenzer for useful discussions and providing their experimental data, and to R. Heinonen for a careful reading of the manuscript. This work was performed under the auspices of the United States Department of Energy under contract DE-AC52-06NA25396.

[1] H. J. Lee *et al.*, Phys. Rev. Lett. **102**, 115001 (2009).
[2] K. Falk, E. J. Gamboa, G. Kagan, D. S. Montgomery, B. Srinivasan, P. Tzeferacos, and J. F. Benage, Phys. Rev. Lett. **112**, 155003 (2014).
[3] S. P. Regan *et al.*, Phys. Rev. Lett. **109**, 265003 (2012).
[4] L. B. Fletcher, A. L. Kritcher, A. Pak, T. Ma, T. Döppner, C. Fortmann, L. Divol, O. S. Jones, O. L. Landen, H. A. Scott, J. Vorberger, D. A. Chapman, D. O. Gericke, B. A. Mattern, G. T. Seidler, G. Gregori, R. W. Falcone, and S. H. Glenzer, Phys. Rev. Lett. **112**, 145004 (2014).
[5] S. H. Glenzer, G. Gregori, R. W. Lee, F. J. Rogers, S. W. Pollaine, and O. L. Landen, Phys. Rev. Lett. **90**, 175002 (2003).
[6] G. Gregori, S. H. Glenzer, F. J. Rogers, S. M. Pollaine, O. L. Landen, C. Blancard, G. Faussurier, P. Renaudin, S. Kuhlbrodt, and R. Redmer, Phys. Plasmas **11**, 2754 (2004).
[7] S. H. Glenzer, O. L. Landen, P. Neumayer, R. W. Lee, K. Widmann, S. W. Pollaine, R. J. Wallace, G. Gregori, A. Höll, T. Bornath, R. Thiele, V. Schwarz, W.-D. Kraeft, and R. Redmer, Phys. Rev. Lett. **98**, 065002 (2007).
[8] E. G. Saiz *et al.*, Nature Phys. **4**, 940 (2008).
[9] A. L. Kritcher *et al.*, Phys. Rev. Lett. **103**, 245004 (2009).
[10] L. B. Fletcher, H. J. Lee, T. Döppner, E. Galtier, B. Nagler, P. Heimann, C. Fortmann, S. LePape, T. Ma, M. Millot *et al.*, Nature Photonics **9**, 274 (2015).
[11] T. Ma, T. Döppner, R. W. Falcone, L. Fletcher, C. Fortmann, D. O. Gericke, O. L. Landen, H. J. Lee, A. Pak, J. Vorberger, K. Wünsch, and S. H. Glenzer, Phys. Rev. Lett. **110**, 065001 (2013).
[12] A. N. Souza, D. J. Perkins, C. E. Starrett, D. Saumon, and S. B. Hansen, Phys. Rev. E **89**, 023108 (2014).
[13] H. R. Rüter and R. Redmer, Phys. Rev. Lett. **112**, 145007 (2014).
[14] J. Clérouin, G. Robert, P. Arnault, C. Ticknor, J. D. Kress, and L. A. Collins, Phys. Rev. E **91**, 011101 (2015).
[15] C. E. Starrett, J. Daligault, and D. Saumon, Phys. Rev. E **91**, 013104 (2015).
[16] G. Chabrier, J. Phys. France **51**, 1607 (1990).
[17] F. J. Rogers, D. A. Young, H. E. DeWitt, and M. Ross, Phys. Rev. A **28**, 2990 (1983).
[18] Y. Rosenfeld, J. Stat. Phys. **42**, 437 (1986).
[19] G. Faussurier, Phys. Rev. E **69**, 066402 (2004).
[20] C. E. Starrett, D. Saumon, J. Daligault, and S. Hamel, Phys. Rev. E **90**, 033110 (2014).
[21] C. E. Starrett and D. Saumon, High Energy Dens. Phys. **10**, 35 (2014).
[22] C. E. Starrett and D. Saumon, Phys. Rev. E **87**, 013104 (2013).
[23] V. V. Karasiev, T. Sjostrom, J. Dufty, and S. B. Trickey, Phys. Rev. Lett. **112**, 076403 (2014).
[24] J.-F. Danel, L. Kazandjian, and G. Zérah, Phys. Plasmas **13**, 092701 (2006).
[25] N. M. Gill, R. A. Heinonen, C. E. Starrett, and D. Saumon, Phys. Rev. E **91**, 063109 (2015).
[26] T. Ott, M. Bonitz, L. G. Stanton, and M. S. Murillo, Phys. Plasmas **21**, 113704 (2014).
[27] J. Chihara, J. Phys.: Condens. Matter **12**, 231 (2000).
[28] S. H. Glenzer and R. Redmer, Rev. Mod. Phys. **81**, 1625 (2009).
[29] D. O. Gericke, J. Vorberger, K. Wünsch, and G. Gregori, Phys. Rev. E **81**, 065401 (2010).
[30] K. Wünsch, J. Vorberger, and D. O. Gericke, Phys. Rev. E **79**, 010201(R) (2009).
[31] D. Saumon, C. E. Starrett, J. A. Anta, W. S. Daughton, and G. Chabrier, in *Frontiers and Challenges in Warm Dense Matter*, Lecture Notes in Computational Science and Engineering, Vol. 96 (Springer, New York, 2014), p. 151.
[32] J. Clérouin, G. Robert, P. Arnault, J. D. Kress, and L. A. Collins, Phys. Rev. E **87**, 061101(R) 2013.
[33] P. Arnault, J. Clérouin, G. Robert, C. Ticknor, J. D. Kress, and L. A. Collins, Phys. Rev. E **88**, 063106 (2013).
[34] G. Faussurier and C. Blancard, Phys. Rev. E **91**, 063104 (2015).
[35] L. E. Gonzalez, D. J. Gonzalez, and M. Silbert, Phys. Rev. A **45**, 3803 (1992).
[36] L. E. Gonzalez, D. J. Gonzalez, and M. Silbert, Physica B **168**, 39 (1991).